Polymer 134 (2018) 44–52

Contents lists available at ScienceDirect

Polymer

journal homepage: www.elsevier.com/locate/polymer

Synthesis and characterization of a new poly(dithieno (3,2-b:2′, 3′-d) pyrrole) derivative conjugated polymer: Its electrochromic and biosensing applications

Hacer Azak [a], Huseyin Bekir Yildiz [b, c, *], Buket Bezgin Carbas [d, e, **]

[a] Department of Chemistry, Karamanoglu Mehmetbey University, 70100 Karaman, Turkey
[b] Department of Materials Science and Nanotechnology Engineering, KTO, Karatay University, Karatay, 42020 Konya, Turkey
[c] Biotechnology Research Lab, FELSIM Inc, Konya Technocity, Selcuklu, 42003 Konya, Turkey
[d] Department of Energy Systems Engineering, Karamanoglu Mehmetbey University, 70100 Karaman, Turkey
[e] Conductive Polymers and Energy Applications Laboratory, Karamanoglu Mehmetbey University, 70100 Karaman, Turkey

ARTICLE INFO

Article history:
Received 18 October 2017
Received in revised form
16 November 2017
Accepted 20 November 2017
Available online 22 November 2017

Keywords:
Electrochromism
Enzyme immobilization
Dithieno[3,2-b:2′,3′-d]pyrrole

ABSTRACT

Synthesis and electropolymerization of a new conjugated dithieno(3,2-b:2′,3′-d) pyrole (DTP) derivative, namely, 2-(2-(2-(4H-dithieno[3,2-b:2′,3′-d]pyrrol-4-yl)ethoxy)ethoxy)ethanamine, (DTP-alkoxy-NH_2) monomer are presented. The electrochemical, spectroelectrochemical effects and biosensor capability towards to glucose oxidase enzyme of P(DTP-alkoxy-NH_2) polymer film are investigated in detail during the placement of alkoxy-NH_2 functional unit in the polymer. Electrochemical and optical results between neutral and oxidized states of the polymer film show that (P(DTP-alkoxy-NH_2)) has reversibly multi-electrochromic behaviors. Furthermore, glucose oxidase enzyme (GOx) is covalently immobilized on Au electrodes modified with P(DTP-alkoxy-NH_2) conducting polymer. This enzyme is entrapped into conducting polymer during electropolymerization of DTP monomer on the electrodes. Some characterization parameters (Maximum reaction rate, Michaelis–Menten constants, temperature, pH and operational stabilities) for this kind of biosensor application is also determined.

1. Introduction

Conducting polymers based on thiophene and pyrrole monomers, which both are incorporated in the same main chain backbone, have been continuing to attract researcher's interest in recent years due to their low oxidation potential, high electrical conductivities and environmental stability in their redox states [1]. Meanwhile, the dithieno[3,2-b:2′,3′-d]pyrrol (DTP) based conjugated organic materials have been precursor materials because their chemical structure with strong electron donating ability promises easily functionalization for polymers [2–14]. Different unit substitution from pyrrole unit in excellent molecular DTP structures has been bringing a breath of fresh air to the field of conjugated polymer since thiophene-pyrrole-thiophene comonomer structure has a fused ring system and good planar structure, which make an extended conjugated polymer during electropolymerization step [4,15,16]. For that reason, a remarkable amount of research effort has been committed to synthesize and create applications of novel DTP based conjugated polymers. The corresponding polymers of DTP moieties have been used in optoelectronic devices energy storage applications, biosensors and electrochromic display applications [2,3,17–23]. However, up to now, very few electrochromic homopolymers based on DTP systems have been introduced into literature [2,16,23]. First pioneering studies of electrochromic DTP systems, which were prepared in order to get low band gap processable polymers, were reported by Berlin et al. [2] and Rasmussen et al. [16]. The polymers show redox active behavior and excellent electrochromic properties (red color at the neutral state and blue at the oxidized states). Our group were also divided the DTP derivatives into three groups (first, second and new generation DTP) depending on the N-functionalized groups. The results show that new generations DTP derivatives had better properties compared to other electrochromic DTP derivatives [23].

* Corresponding author. Department of Materials Science and Nanotechnology Engineering, KTO, Karatay University, Karatay, 42020 Konya, Turkey.
** Corresponding author. Department of Energy Systems Engineering, Karamanoglu Mehmetbey University, 70100 Karaman, Turkey.
E-mail addresses: huseyinbekir.yildiz@karatay.edu.tr (H.B. Yildiz), bcarbas@kmu.edu.tr (B. Bezgin Carbas).

https://doi.org/10.1016/j.polymer.2017.11.044
0032-3861/

Based upon these experiences for DTP based polymers, we have launched a new route, which has a purpose of design and synthesize of new electrochromic processable DTP based polymeric materials functionalized from N position of pyrrole ring.

Another important application area of conjugated polymers is biosensors, which have gained ever-increasing acceptance in literature because of their facile recognition for many significant analytes in biological systems [18–24]. Biosensors are analytical devices containing a biological analyte recognition element and a transducer that changes biochemical signal into electrical one, and signal display unit. Conducting polymers have been using for making electrochemical biosensors due to their high electrical conductivity property resulting from electrochemical redox activity and charge transfer rate next to the chemical properties. These properties make also the conducting polymers as an outstanding immobilization platform for biological elements [33–39]. There are some enzyme immobilization methods (adsorption, covalent bonding, entrapment and crosslinking) in order to make a success of the loss of enzyme on a support surface, enzyme stability and shelf life for biosensors [25,26]. If conjugated polymers are designed depending on the biological molecule, they can provide a proper microenvironment matrices and fast electron transition between biomolecule and conjugated polymer for immobilization [27–32]. Among conjugated polymers, DTP based polymers provide tailor made molecular design for biosensors. Polymeric conducting DTP derivatives are becoming prominent as useful structures for both molecular and polymeric materials in the biosensor design due to their planar structures, fused ring systems, electron releasing groups, and conjugation properties to increase the electron transfer rate in the enzyme based biosensors. By using these properties difficulty of the direct electron transfer between enzyme and the electrode has been overcome easily and they play a key role in the design and fabrication of biosensors [33]. Another advantage of these materials is their simple and low-cost processing as well as their potential for electronic, optoelectronic and biosensing applications. Therefore, if all the advantages of DTP type conducting polymers are considered, it can be thought that it is thought they can be effectively used in biosensors and their application to the fabrication of biosensors is useful [33,34]. Recent years, there are some studies related with biosensor applications of DTP based conjugated polymers. The charge transport property during p-doping, tunable optical properties, stability and biocompatibility properties of amine functionalized DTP polymers make the system suitable for the fabrication of biosensor applications [37–41].

Herein, we wish to report a new monomer and its corresponding electrochromic polymer, namely, poly(2-(2-(2-(4H-dithieno[3,2-b:2′,3′-d]pyrrol-4-yl)ethoxy)ethoxy)ethanamine) (P(DTP-alkoxy-NH_2)) for biomolecule immobilization. Electrochromic and electrochemical biosensor applications of a novel DTP-typed polymer formed by electrochemical polymerization of the monomers were also investigated in detail.

2. Experimental section

All chemicals were purchased from Sigma Aldrich, Across and used as received unless otherwise noted. 2-(2-(2-(4H-dithieno[3,2-b:2′,3′-d]pyrrol-4-yl)ethoxy)ethoxy)ethanamine, (DTP-alkoxy-NH_2) was synthesized according to Scheme 1.

2.1. Synthesis of 2-(2-(2-(4H-dithieno[3,2-b:2′,3′-d]pyrrol-4-yl) ethoxy)ethoxy)ethanamine, (DTP-alkoxy-NH_2)

3,3′-dibromo-2,2′-bithiophene (100 mg, 0.31 mmol) (2) and 2,2'-(ethane-1,2-diylbis(oxy))diethanamine (53 mg, t-BuONa (65 mg, 0.67 mmol), $Pd_2(dba)_3$ (14 mg, 0.02 mmol) and BINAP (14 mg, 0.02 mmol) in dry toluene (4 ml) were mixed under nitrogen atmosphere and stirred for 20 min at room temperature. The reactants were heated under reflux until starting chemicals were consumed (monitored by TLC). The reaction medium was cooled for 1 h. The water was added in to reaction mixture and organic and inorganic layers were separated with extraction method (twice with EtOAc (2 × 30 mL)-water mixture). Organic phase was dried over MgSO4 and filtered, evaporated and purified. The crude product was silica gel (20 g) eluted with methanol from the column. The brown solid was obtained (Scheme 1). Recrystallization from dichloromethane/hexane afforded yellow crystals (Yield 45%). ^{1}H NMR (400 MHz, $CDCl_3$, δ): 7.13 (d, $J = 5.3$ Hz, 2H) 6.98(d, $J = 5.3$ Hz, 2H), 4.4–2.8 (m, 12H). ^{13}C NMR (100 MHz, $CDCl_3$, δ): 144.17, 123.35, 114.58, 111.65, 59.7, 42.4, 32.7, 29.4, 29.3, 29.3. The solution of DTP-alkoxy-NH_2 in DCM had two absorption peaks at 234 nm and 297 nm.

2.2. Electropolymerization of P(DTP-alkoxy-NH_2)

Monomer was electropolymerized by using cyclic voltammetry (CV) method. A simple three electrode system was used and this set up contains indium tin oxide (ITO)-coated glass as working electrode, Pt wire as counter electrode and Ag wire as reference electrode for electroanalytical characterizations and electropolymerization steps. As electrolyte medium, 0.1 M tetrabutyl ammonium hexafluorophosphate ($TBAPF_6$) in acetonitrile (ACN) was used during electropolymerization and electrochemical characterizations of polymer. For electropolymerization step, 10 mM monomers concentration were added into electrolyte medium and scanned potentials between proper range specified for each polymer for 25 cycles. Polymer films were cleaned with ACN solvent in order to get rid of unreacted monomers or oligomeric species.

2.3. Chemical structure, morphological, electrochemical and optical characterization of P(DTP-alkoxy-NH_2)

Chemical structure of monomers was depicted by using NMR and FTIR spectra. NMR spectra were recorded with a Bruker NMR spectrometer at 400 MHz for ^{1}H NMR and 100 MHz ^{13}C NMR in $CDCl_3$. FTIR spectra of both monomers and polymers were recorded with a Bruker Vertex 70 Spectrophotometer. Ivium compactstat potenstiostat was used for electroanalytical measurements. For optical and spectroelectrochemical studies, a Specord S600 spectrometer was used and color spaces of electrochromic analysis were also done. The color data given by the International Commission of Illumination with luminance (L), hue (a), and intensity (b). AFM imaging of polymer films were done with a Nanomagnetics Instruments under ambient laboratory conditions. For optical studies, a different cell design was used. It consists of a quartz cuvete with a 1 cm path length and optically transparent working electrode (indium-tin oxide (ITO, Delta. Tech. 8–12 Ω, 0.7 × 5.0 cm^2). A Pt and an Ag wires were used as counter and pseudo reference electrodes, respectively for optical analysis of polymer. Electropolymerization procedure was applied by using cyclic voltammetry technique for both electrodes. After polymerization procedure, the working electrode ITO was cleaned with ACN solvent. Square wave potential and CV techniques were used in order to investigate the switching ability and optical properties at different redox potentials upon oxidation.

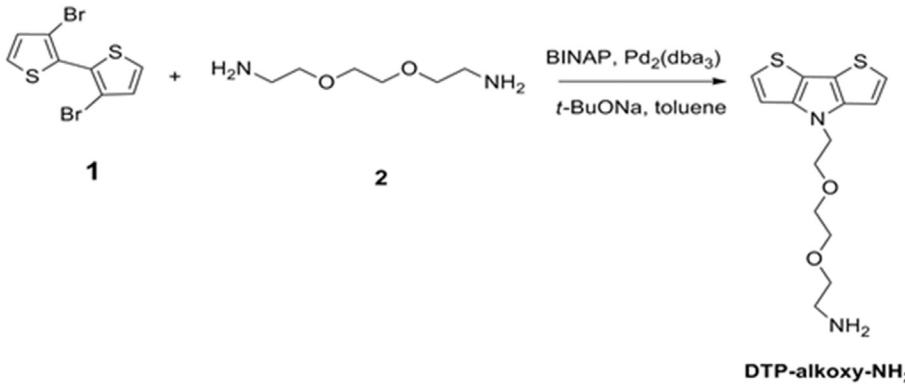

Scheme 1. Synthesis route of DTP-alkoxy-NH_2 monomer.

2.4. Biosensor application of P(DTP-alkoxy-NH2)

Before each experiment, the gold electrodes were polished with wet emery paper and rinsed thoroughly with distilled water. A DTP-alkoxy-NH_2 layer covered gold electrode was used to immobilize GOx. The polymer coatings were formed on the working electrode by using 25 voltammetric cycles between 1.0 V and −1.0 V at a scan rate of 0.1 V s^{-1} in a ACN solution containing 10 mM DTP-alkoxy-NH_2 monomer, 0.1 M $TBAPF_6$ supporting electrolyte. For the immobilization of the enzyme, proper amounts of a GOx solution (1.0 mg in 5.0 mL, 50 mM sodium phosphate buffer, pH 7.0) and glutaraldehyde solution (5.0 mL, 1.0% in sodium phosphate buffer, pH 7.0) were spread over the polymer-coated gold electrodes. Then, the electrodes were allowed to stand at ambient conditions for 90 min. The daily prepared P(DTP-alkoxy-NH2)/GOx biosensors were used in all experiments. A schematic representation of the P(DTP-alkoxy-NH_2)/GOx biosensors is shown in Scheme 2.

Three electrode system including a graphite rod (d = 5 mm) counter electrode, calomel reference electrode and gold working electrode was used. All electrochemical experiments were carried out using an electrochemical analyzer with potentiostat (EG&G Model 263). Amperometric experiments were examined in room temperature (25 °C) using 10 mL, 50 mM phosphate buffer. The current density was calculated with the oxygen consumption after adding glucose under −0.7 V. Calibration curves were obtained by plotting photocurrent vs. substrate concentration and y = mx + n equations were obtained where y is the sensor response in current (nA) and x is the substrate concentration. Limit of detection (LOD) was calculated from the equations of LOD = 3S/N using the standard deviation of response (s) and the slope of the calibration curve. The proposed amperometric biosensors were tested to analyze glucose in spiked human serum. No sample pretreatment was required for the analysis. Known amount of glucose and acetonitrile was added to the human serum samples and it was ultrasonicated for 10 min at 2500 rpm. Supernatant part was taken and glucose response was recorded for different concentration. The glucose detection from human serum (human male AB plasma) was achieved by recovery tests after addition of known amounts of glucose to the human serum plasma and dilution with phosphate buffer. Applicability of the proposed method was confirmed by utilizing recovery studies in spiked human serum analyses [33]. The reaction temperature was changed between 10 °C and 60 °C while the cholesterol concentration was kept constant at 10 Km for every case. For pH optimization at 25 °C, (in order to be able to use these electrodes as biosensors) the pH of the reaction was altered between pH 4 and pH 11 while the glucose concentration was kept constant at 10 Km. In all experiments for both pH and temperature optimizations, the enzyme activity determination experiments were performed via application of −0.7 V as previously described in the measurements section. Relative enzyme activity was calculated by assigning the maximum value of activity as 100% in determination of optimum pH and temperature experiments. The operational stability of electrodes was studied by performing 40 repetitive measurements in the same day. Storage stability of

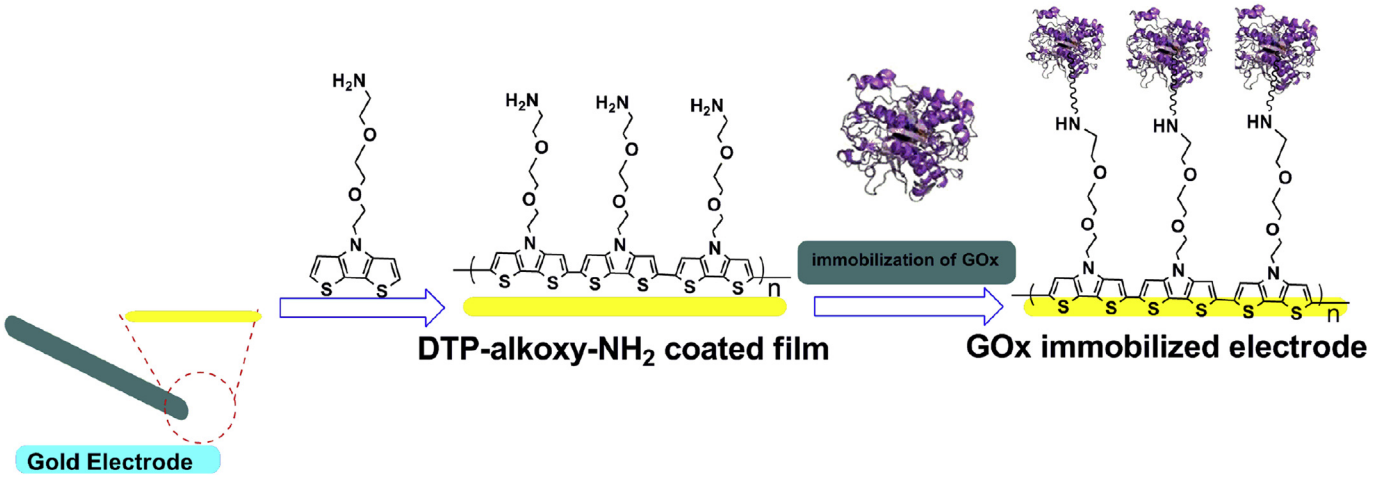

Scheme 2. Schematic illustration of preparation of GOx immobilized biosensing electrode.

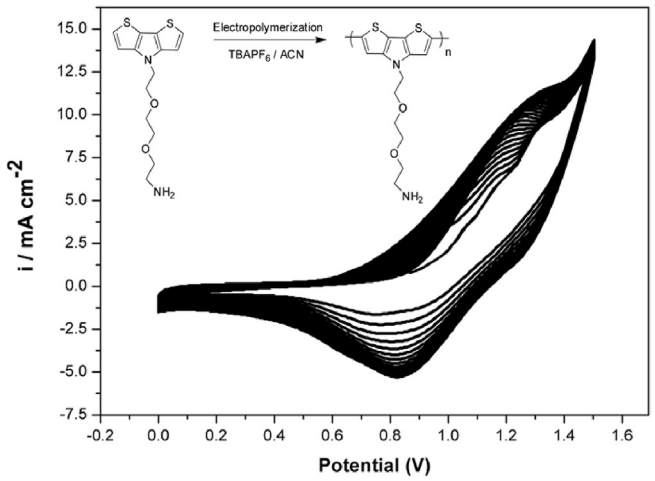

Fig. 1. Cyclic voltammograms of DTP-alkoxy-NH_2 monomer in $TBAPF_6$/ACN medium with a scan rate of 100 mV s^{-1}.

enzyme electrodes was determined by checking the activities every day for a week and then once in 5 days throughout 40 days. In the investigations of both operational and storage stabilities, enzyme activity determination was found via application of −0.7 V at pH 7.0 and 25 °C as previously described in the measurements section. Substrate concentrations were kept at 10 Km and electrodes were stored in buffer solution at 4 °C when not in use. As done in determination of optimum pH and temperature experiments, relative enzyme activity was calculated by assigning the maximum values of activity as 100% in operational and storage stability experiments.

3. Results and discussion

The electrochemical polymerization of DTP-alkoxy-NH_2 was synthesized via CV electroanalytical method. Fig. 1 shows repetitive cyclic voltammograms of P(DTP-alkoxy-NH_2) in the presence of $TBAPF_6$/ACN solution at a scan rate of 100 mV s^{-1}. A concentration of 10 mM monomer, 0.1 M $TBAPF_6$ supporting electrolyte and ACN were found suitable for electropolymerization of the monomer. The monomer oxidation of DTP-alkoxy-NH_2 occurred at 1.27 V versus

Table 1
Electrochemical and optical data for DTP based monomers and their polymers in the literature.

Chemical Structures	E^{ox}_{mon} (V)	$E^{onset\ ox}_{pol}$ (V)	HOMO* (eV)	LUMO (eV)	E^{opt}_{pol} (V)	λ_{max} (nm)	Optical Contrast (%)	Switching time (s)
DTP = 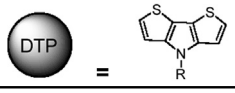								
R = -$C_{10}H_{20}$-NH_2	**1.30**	**0.35**	**−5.45**	**−3.45**	**2.00**	**475**	**35**	**0.7**
DTP-alkyl-NH_2	vs.	vs. Ag wire				**1030**	**50**	**0.9**
[23]	Ag wire							
DTP-alkoxy-NH_2	**1.27**	**0.45**	**−5.55**	**−3.63**	**1.92**	**420**	**9.0**	**1.8**
This work	vs.	vs.				**770**	**24**	**1.0**
	Ag wire	Ag wire				**980**	**30**	**0.8**
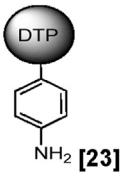	**1.25**	**0.50**	**−5.60**	**−3.95**	**1.65**	**410**	**14**	**1.8**
	vs.	vs.				**1060**	**32**	**1.5**
	Ag wire	Ag wire						
DTP-aryl-NH_2								
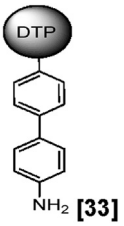	**1.10**	-	-	-	-	-	-	-
	vs.							
	Ag wire							
DTP-Ph-Ph-NH_2								
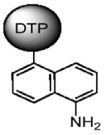	**0.50**	-	-	-	-	-	-	-
	vs. Ag/AgCl							
DTP-NH_2 [35]								

The highest occupied molecular orbital (HOMO) energy levels were calculated according to normal hydrogen electrode value as −4.75 eV. * HOMO = $-(4.75 + 0.35 + E^{onset\ ox}_{pol})$

where $E^{onset\ ox}_{pol}$ onset oxidation potential.

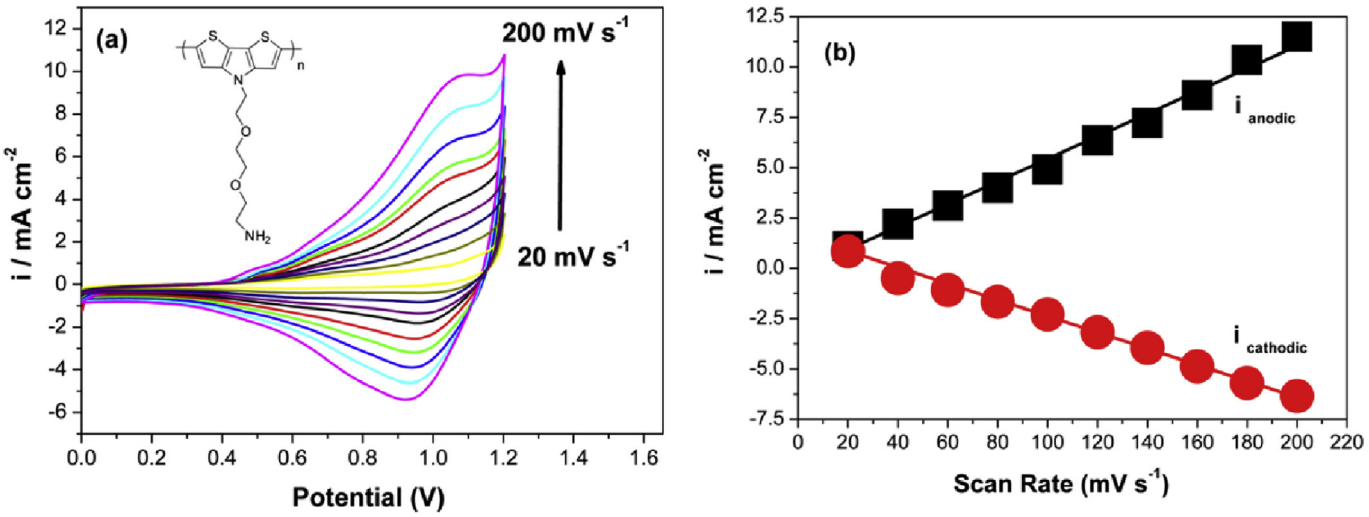

Fig. 2. **(a)** p-Type doping behavior of P(DTP-alkoxy-NH_2) film **(b)** relationship of anodic (i_{anodic}) and cathodic current ($i_{cathodic}$) peaks at various scan rates in 0.1 M $TBAPF_6$/ACN.

Ag wire. The increase of the current value in the new cycle after the monomer is oxidized, indicating the formation of P (DTP-alkoxy-NH_2), which is covered by an electroactive polymer film electrode surface on the electrode surface.

The voltammetric and optical data for DTP based monomers and their polymers in literature were summarized in Table 1. As shown in Table 1, The monomer oxidation potential of DTP-alkoxy-NH_2 was higher than those of DTP-Ph-Ph-NH_2 [33], DTP-NH_2 [35], DTP-aryl-NH_2 [23] and lower than those of DTP-alkyl-NH_2 [23]. While electron delocalization contribution of the aryl units in the system lowers the oxidation potential of monomers (DTP-Ph-Ph-NH_2 [33], DTP-NH_2 [35],DTP-aryl-NH_2 [23]) the DTP structures with alkoxy and alkyl units have approximately same oxidation potential. Alkoxy usage in the structure (DTP-alkoxy-NH_2) makes a little bit easier electron oxidation of the monomer than that of DTP-alkyl-NH_2 because of the electron donating effect of the alkoxy unit.

3.1. Electrochemical characterization of P(DTP-alkoxy-NH_2)

The electrochemical behavior of polymer film was investigated in monomer free electrolytic solution. The polymer film coated on the working electrode surface was analyzed via cyclic voltammetry method between neutral and oxidized states at various scanning rates (Fig. 2a). The anodic (i_{anodic}) and cathodic ($i_{cathodic}$) current values were investigated in Fig. 2b depending on the scanning rate. It has been observed that both the anodic and cathodic peaks increase linearly with the increase of scanning rate. This suggests that the redox process is non-diffusional and the polymer film is very well coated on the working electrode surface. As shown in Table 1, the onset oxidation potential of the polymers decreased in the order P(DTP-aryl-NH_2) [23]> P(DTP-alkoxy-NH_2) > P(DTP-alkyl-NH_2) [23].

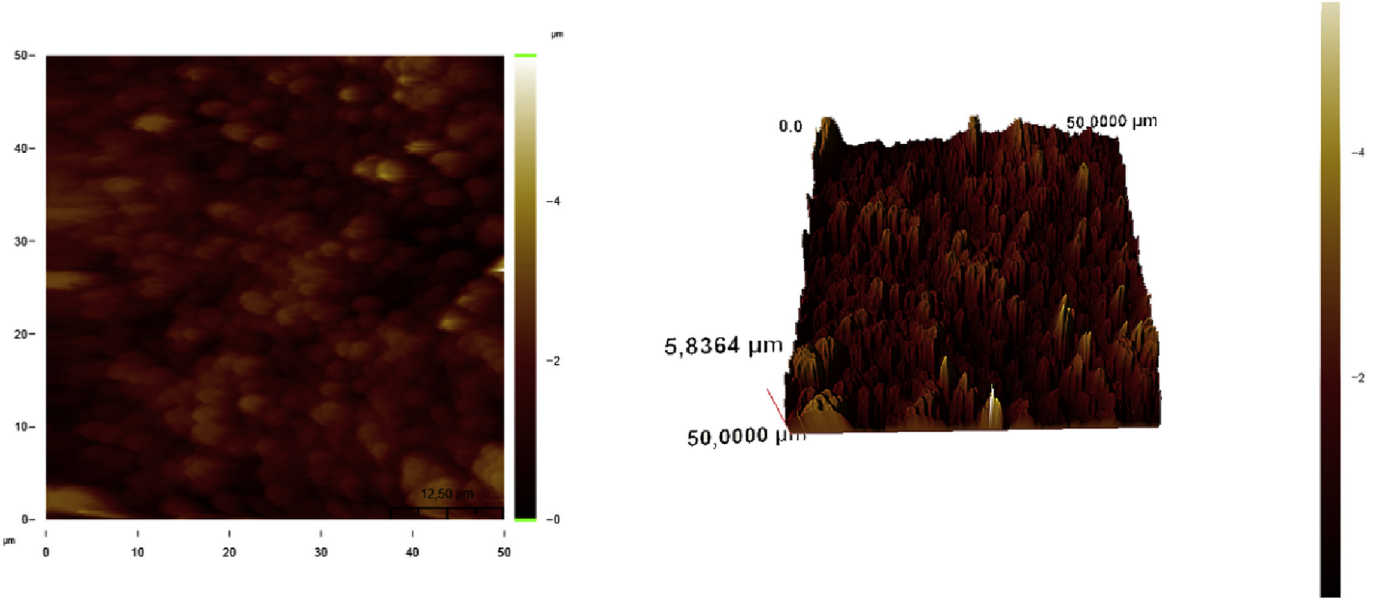

Fig. 3. Topological surface and 3D images AFM images of P(DTP-alkoxy-NH_2).

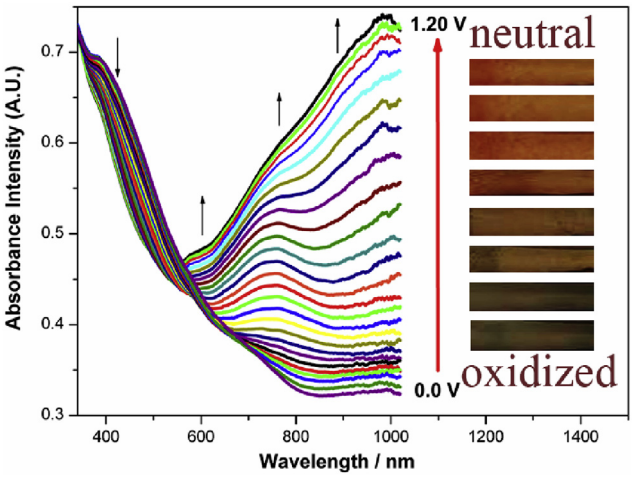

Fig. 4. Spectroelectrochemical behavior of P(DTP-alkoxy-NH_2).

3.2. Morphological and chemical structure analysis

Polymer film formation has also been proved by FTIR spectroscopy. While most characteristic peaks of the monomer remained the same, the peak at 692 cm^{-1} of the monomer completely disappeared after polymerization and a new peak of dopant at 833 cm^{-1} appeared which indicates the presence of dopant anions PF_6^-. Polymer film morphology coated on ITO electrode was analyzed by AFM technique. Fig. 3 shows the two-dimensional and three-dimensional state AFM image of the polymer film. As you can see, the surface of the polymer film is very rough with globular morphology (peak to peak (Rt) = 2.58 μm RMS = 0.26 μm). Such surfaces are very important for the redox activity of the polymer because the surface morphology facilitates to move counter ions easily into and out of the polymer film during doping and dedoping processes.

3.3. Spectroelectrochemical and optical properties

The spectroelectrochemical behavior of the P(DTP-alkoxy-NH_2) polymer film was made in order to interpret electronic transitions during doping and dedoping of polymer. P (DTP-alkoxy-NH_2) coated on ITO film was scanned with a cyclic voltammeter at a potential range of 0.0 V and 1.2 V, while optical data were taken with a UV–vis spectrophotometer as seen in Fig. 4. As the potential value increases, the π -π * band (at 420 nm) decreases and the bands increases to about 0.4 V at 770 nm, after which the new band increases to 980 nm upon oxidation. These transitions have shown that new load transition bands are formed between the valence and the conduction bands.

Spectroelectrochemical and electrochemical studies are important to get an idea of the polymer band gap. Finding the HOMO and LUMO energy levels of the polymer is also very important in the field of material application science. The optical band gap is calculated from the starting point of the π -π * electronic transition from the data in the UV–vis spectrum. The polymer band gap was calculated as 1.92 eV. When compared other DTP derivatives, as seen in Table 1, the band gaps of alkyl and alkoxy DTP derivative polymer films have approximately same value (~2.0 eV), which is higher than that of P(DTP-aryl-NH_2). HOMO level of polymer film is calculated from the onset of polymer film oxidation. The LUMO level is found by subtracting the HOMO level from the optical band gap. While the HOMO level was found as −5.55 eV, the LUMO level has an energy level as −3.63 eV. While the HOMO levels of the polymers had the approximately same value, The LUMO levels had different energy values depending on the band gap value of corresponding polymers.

Colorimetric analyzes are very important to determine the color of electrochromic polymers. Color coordinates are very important for universal identification of colors. According to the color change upon oxidation, the colors were determined according to CIE 1976 (L, a, b) color space with daylight (Standard Illuminant D65/10 as illuminant and 10°), where L is the parameter of the lightness, a is the red-green balance and b is yellow-blue balance. There are three important parameters to promote colors. Brightness (L), color tone (a), and saturation (b). The values of L, a, b are given in Table 2. As seen in Table 2, the polymer film shows the behavior of multichromic polymer film. The polymer film has reddish orange and dark blue colors in the neutral and oxidized state, respectively. Furthermore, it has brown color at 0.6 V in the intermediate state of polymer films.

The polymer film switching ability is obtained by varying the T% (percent transmittance) value while the polymer film is in a neutral and oxidized state while a constant wavelength is selected. The results are summarized in Fig. 5a and b. The electrochromic contrast ratio was found to be 24% and 30% at 770 nm and 980 nm, respectively. The optical contrast value in the neutral state was

Table 2
Electrochromic colors of P (TCP) films at various potentials and their corresponding data related color scale.

Applied Potential	0.0 V	0.1 V	0.2 V	0.4 V	0.6 V	0.8 V	1.0 V	1.1 V	1.20 V
Colours									
L	108.2	105.8	104.3	87.5	68.8	61.2	51.1	60.1	64.4
a	71.3	68.7	55.8	59.7	55.5	47.5	49.3	49.4	55.1
b	44.5	41.1	34.3	37.2	38.7	34.6	37.4	39.8	43.3

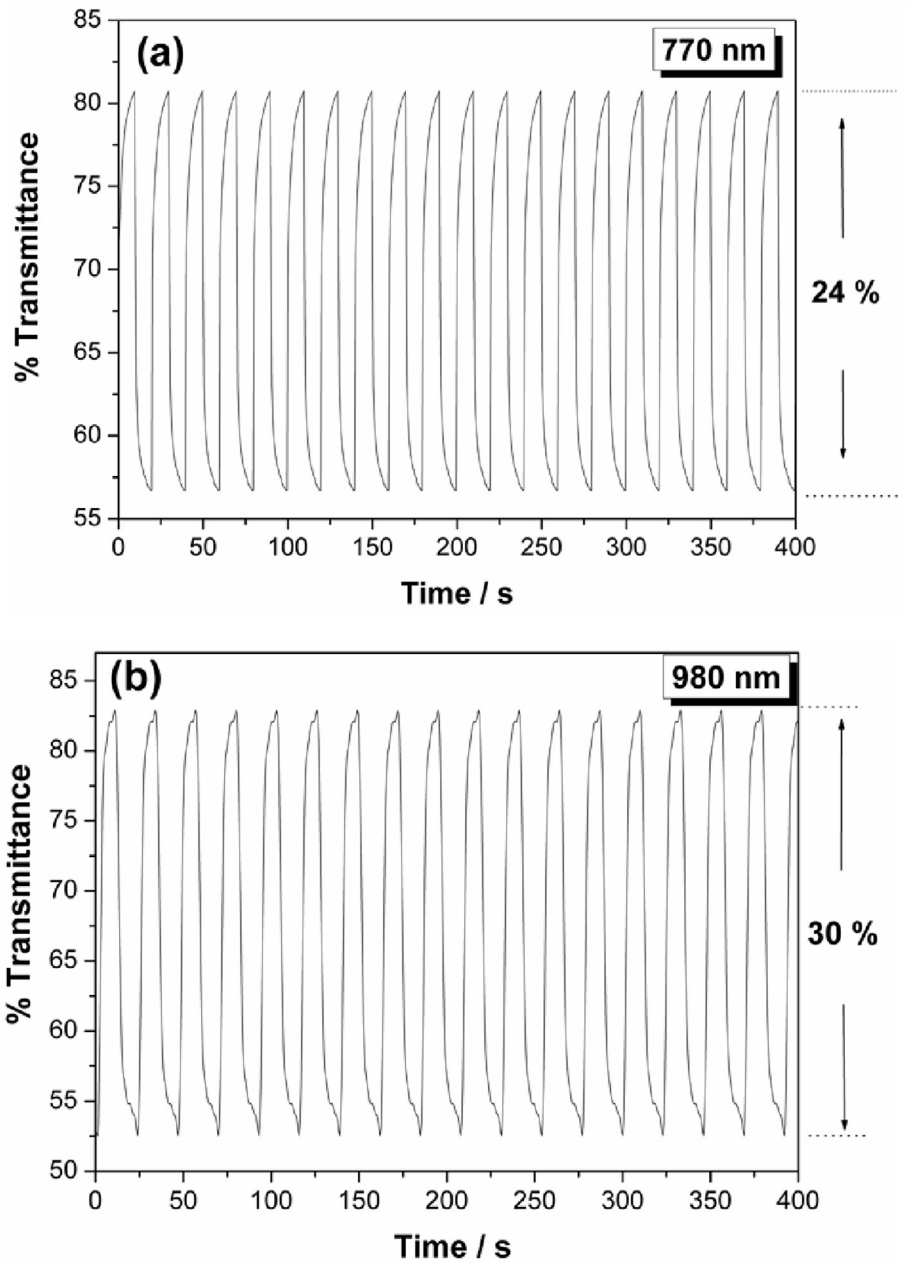

Fig. 5. Investigation of electrochromic switching propertyof P (DTP-alkoxy-NH_2) polymer **(a)** at 770 nm and **(b)** at 980 nm.

found as 9.0 at 420 nm. Switching speeds were found for approximately 1.8 s at 420 nm, 1.0 s at 770 nm and 0.8 s at 980 nm. As noted in Table 1, the optical contrast and switching time values of the DTP polymer derivates change depending on the functional substituted structure (-alkyl, -alkoxy and −aryl) in the polymer chain.

3.4. Preparation and optimization of the biosensors

3.4.1. Analytical characterization of the biosensors

Analytical characterization of the P(DTP-alkoxy-NH_2)/GOx biosensor was achieved by obtaining linear dynamic ranges and the equations at the optimized electrode configuration with LOD and LOQ values, and standard error values of slope and intercepts. For the proposed systems, linear calibration graphs and their photocurrent action spectra were given in Fig. 6. For P(DTP-alkoxy-NH_2)/GOx enzyme electrode, the linear relation was observed in the range of 0.05–0.9 mM glucose and defined by the equation; $y = 95.24x + 7.76$ ($r^2 = 0.998$). LOD value for P(DTP-alkoxy-NH_2)/GOx electrode was obtained as 3.48 × 10-4 mM glucose according to S/N = 3 ratios. LOQ value for P(DTP-alkoxy-NH_2)/GOx electrode was obtained as 1.05×10^{-3}mM respectively according to S/N = 10 ratios (n = 4).

Kinetic parameters for the amperometric biosensors include the maximum reaction rate (I_{max}) of the enzymatic reaction and the Michaelis-Menten constant (Km) which is the equilibrium dissociation constant for the complex. The Michaelis-Menten constant (Km), defines the affinity of enzyme toward its substrate corresponds to substrate concentration at ½ Imax [42]. The lower the Km value means the higher its affinity against its substrate. The kinetic parameters, I_{max} and Km, were obtained from the Lineweaver-Burk plot which is a plot of 1/Vo against 1/[Substrate] for systems

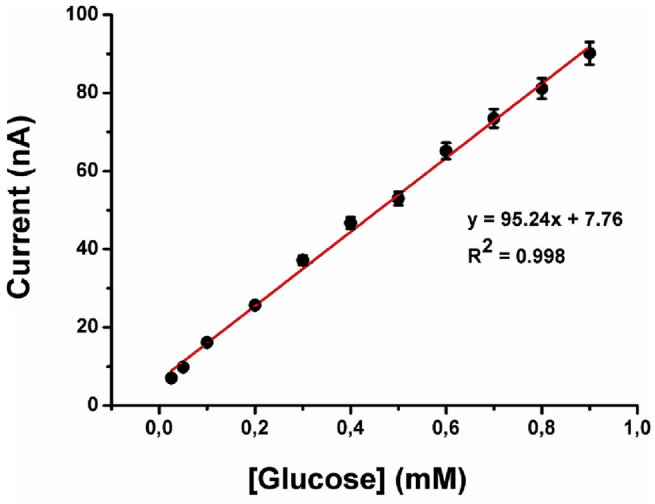

Fig. 6. Calibration curves for the detection of glucose (in a pH 7.0 buffer, 0.1 M, −0.7 V).

obeying the Michaelis-Menten equation. The graph being linear can be extrapolated at anywhere approximating to a saturating substrate concentration, even if no experiment has been performed and from the extrapolated graph, the values of Km and V_{max} can be determined. Maximum velocity (Imax) and Michaelis–Menten constants (Km) for P(DTP-alkoxy-NH_2)/GOx biosensor were calculated as 305.6 $nAcm^{-2}$ and 2.21 mM respectively. A comparison of the analytical performance of the conducting polymer-based glucose biosensors is shown in Table 3.

3.4.2. Application of DTP-alkoxy-NH_2 in biosensor constructions

3.4.2.1. Effects of temperature and pH. The enzyme activity strongly depends on temperature because very hot or very cold conditions can inactivate the enzyme. The temperature stabilities of the freshly prepared enzyme electrodes were determined via application of −0.7 V at different temperatures ranging from 10 to 60 °C in phosphate buffer (pH 7.0) while glucose concentration was kept constant at 10 Km for every case. The maximum activity was observed at 30 °C for free [43]. As illustrated in Fig. 7a, current response gradually increased with increasing temperature and reached amaximum at 50 °C. This biosensor also showed 65% relative activity even at the lowest temperature of 10 °C Therefore, it can be said that this enzyme electrode can be used safely at low temperatures. The buffer pH is an influential parameter for enzymes to sustain their maximum activity and catalysis efficiency. In order to optimize pH, for Poly(DTP-alkoxy−NH_2) GOx biosensor pH dependence experiments were performed over the range of pH 4.0–12.0 in the 50 mM phosphate buffer solution with an applied potential of 0.7 V. As it can be seen from Fig. 8b the maximum peak current of the biosensor was observed at pH 7.0. Thus, 50 mM phosphate buffer pH 7.0 was selected as the optimum for subsequent experiments.

3.4.2.2. Operational and storage stability. Enzymes can easily lose their catalytic activity and denatured. Biomolecules like enzymes have limited stabilities especially when they are removed from their native areas and their stabilities and performances decrease due to immobilization. Therefore operational and storage stability are important considerations for biosensors. Operational and storage stabilities were shown in Fig. 8a and b, respectively. Operational stability of enzyme electrodes was tried to estimate the stability of electrodes in terms of 40 repetitive uses. P(DTP-alkoxy-NH_2)/GOx

Table 3
Some features of conducting polymer-based biosensors in the literature.

Electrode	Conducting Polymer	Principle of detection (working potential)	Linearity for glucose	LOD	Ref.
GE	DTP-NH_2	CA (−0.7 V)	0.05–1.0 mM	5 μM	[35] (Batch)
GE	DTP-NH_2	CA (−0.7 V)	0.1–2.5 mM	64 μM	[35] (FIA)
PGE	DTP-alkyl-NH_2	CA (−0.7 V)	0.3–25 mM	0.074 μM	[36]
Gold E	DTP-Ph-NH_2/GOx/AuNP	CA (−0.7 V)	0.1–2.5 mM	5.00×10^{-2}mM	[33]
Gold E	DTP-Ph-Ph-NH_2/AuNP/GOx	CA (−0.7 V)	0.05–1.0 mM	9.86×10^{-2} μM	[33]
GE	SNS-NH_2/AuNP	CA (−0.7 V)	0.002–5.0 mM.	2.1 μM	[38]
GE	PBDT	CA (−0.7 V)	0.05–2.0 mM	50 μM	[39]
GE	PESeE	CA (−0.7 V)	0.01–2.0 mM	10 μM	[39]
Pt E	GOx/PtNP/PA	CA (+0.56 V)	0.01–8 mM	0.7 μM	[40]
Gold E	DTP-alkoxy-NH_2	CA(-0.7V)	2.0 mM	–	This Work

Abbreviations: CA: Chronoamperometry; GE: Graphite electrode; PGE: Pencil graphite electrode; SNS-NH2: 4-(2,5- di(thiophen-2-yl)-1H-pyrrol-1-yl)benzenamine; AuNP: Gold nanoparticle; PBDT: Poly(4,7-di(2,3)-dihydrothienol[3,4-b][1,4]dioxin-5-yl-benzo[1,2,5]thiadiazole); DTP-NH2:N-functionalized dithienopyrroles; PtNP: Platinum nanoparticles; PA: polyaniline; GOx: Glucose oxidase.

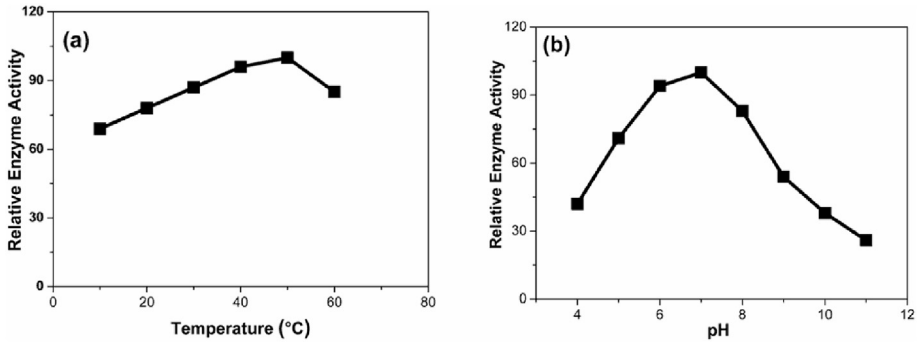

Fig. 7. **(a)** Effect of incubation temperature on activity of glucose oxidase immobilized in P(DTP-alkoxy-NH_2) matrix. **(b)** Effect of pH on activity of glucose oxidase immobilized in P(DTP-alkoxy-NH_2)matrix.

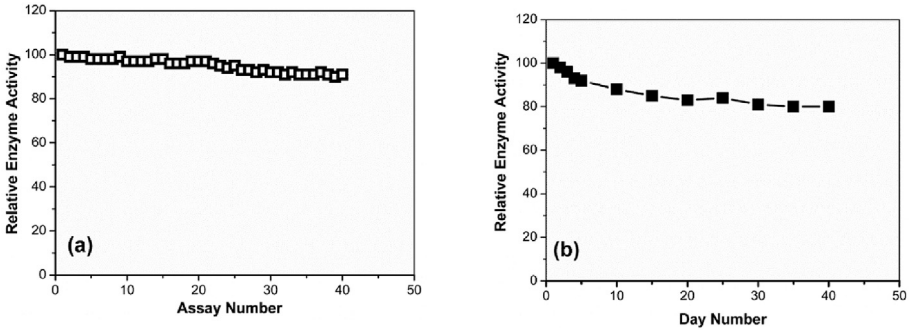

Fig. 8. **(a)** Operational stability of P(DTP-alkoxy-NH_2)/GOx electrode. **(b)** Storage stability of P(DTP-alkoxy-NH_2)/GOx electrode.

electrode exhibited a good stability upon the whole repetitive uses and maintained an activity at 90% until the assay number 40 (Fig. 8a). Storage stability of P(DTP-alkoxy-NH_2)/GOx electrode exhibited an 80% loss of its activity in 20 days and stayed constant until end of the its storage stability experiment (Fig. 8b).

3.4.2.3. Sample application. Glucose amount in spiked human blood samples was tested and recovery analyses were performed to test the accuracy of the designed biosensor. Using P(DTP-alkoxy-NH_2)/GOx biosensor 97.5% recovery was obtained with RSD % value of 0.93%.

4. Conclusions

In this study, the synthesis of 2-(2-(2-(4H-dithieno[3,2-b:2′,3′-d]pyrrol-4 yl)ethoxy)ethoxy)ethanamine, (DTP-alkoxy-NH_2) monomer was successfully achieved. The monomer was electropolymerized and showed multielectrochromic property. A novel amperometric enzymatic biosensors were developed using amine functionalized conducting polymers of 2-(2-(2-(4H-dithieno[3,2-b:2′,3′-d]pyrrol-4 yl)ethoxy)ethoxy)ethanamine (DTP-alkoxy-NH_2) was performed biosensor was easy to prepare and it is useful for glucose detection in batch modes. Represented DTP type conducting polymer can supply a biocompatible and electrochemical microenvironment for immobilization of the enzyme, these immobilization strategies can be light to future researches and could be used in glucose or other important analytes.

Acknowledgements

The author gratefully acknowledges the financial support from Karamanoglu Mehmetbey University (Grant No: 06-M-15).

References

[1] T.A. Skotheim, J.R. Reynolds, in: Handbook of Conducting Polymers – Conjugated Polymers: Synthesis, Properties and Characterization, CRC Press, Boca Raton, FL, 2007, pp. 1–66. Chapter 8.
[2] A. Berlin, G. Pagani, G. Zotti, G. Schiavon, Macromol. Chem. 193 (1992) 399.
[3] K. Ogawa, J.A. Stafford, S.D. Rothstein, D.E. Tallman, S.C. Rasmussen, Synth. Met. 152 (2005) 137.
[4] G. Koeckelberghs, L. De Cremer, A. Persoons, T. Verbiest, Macromolecules 40 (2007) 4173.
[5] W. Vanormelingen, K. Van den Bergh, G. Koeckelberghs, Macromolecules 41 (2008) 5582.
[6] J. Liu, R. Zhang, G. Sauve, T. Kowalewski, R.D. McCullough, J. Am. Chem. Soc. 130 (2008) 13167.
[7] S.P. Mishra, A.K. Palai, R. Srivastava, M.N. Kamalasanan, M. Patri, J. Polym. Sci. Part A Polym. Chem. 47 (2009) 6514.
[8] E. Zhou, M. Nakamura, T. Nishizawa, Y. Zhang, Q. Wei, K. Tajima, C. Yang, K. Hashimoto, Macromolecules 41 (2008) 8302.
[9] M. Nakamura, C. Yang, E. Zhou, K. Tajima, K. Hashimoto, ACS Appl. Mater. Interfaces 1 (2009) 2703.
[10] E. Zhou, K. Tajima, C. Yang, K. Hashimoto, J. Mater. Chem. 20 (2010) 2362.
[11] S. Zhang, Y. Guo, H. Fan, Y. Liu, H.-Y. Chen, G. Yang, X. Zhan, Y. Liu, Y. Li, Y. Yang, J. Polym. Sci. Part A Polym. Chem. 47 (2009) 5498.
[12] W. Yue, Y. Zhao, S. Shao, H. Tian, Z. Xie, Y. Geng, F.J. Wang, Mater. Chem. 19 (2009) 2199.
[13] X. Zhan, Z. Tan, E. Zhou, Y. Li, R. Misra, A. Grant, B. Domercq, X.-H. Zhang, Z. An, X. Zhang, S. Barlow, B. Kippelen, S.R. Marder, J. Mater. Chem. 19 (2009) 5794.
[14] T.T. Steckler, X. Zhang, J. Hwang, R. Honeyager, S. Ohira, X. Zhang, A. Grant, S. Ellinger, S.A. Odom, D. Sweat, D.B. Tanner, A.G. Rinzler, S. Barlow, J.-L. Bredas, B. Kippelen, S.R. Marder, J.R. Reynolds, J. Am. Chem. Soc. 131 (2009) 2824.
[15] M. Parameswaran, G. Balaji, T.M. Jin, C. Vijila, S. Vadukumpully, Z. Forong, S. Valiyaveettil, Org. Electron. 10 (2009) 1534.
[16] K. Ogawa, S.C. Rasmussen, Macromolecules 39 (2006) 1771.
[17] S.J. Evenson, M.J. Mımm, K.I. Pohodya, S.C. Rasmussen, Macromolecules 44 (2011) 835.
[18] G. Balaji, D.I. Phua, W. Shim, S. Valiyaveettil, Org. Lett. 12 (2010) 232.
[19] J. Liu, R. Zhang, G. Sauve, T. Kowalewski, R.D. McCullough, J.Am. Chem. Soc. 130 (2008) 13167.
[20] S.P. Tiwari, J. Kim, K.A. Knauer, D.K. Hwang, L.E. Polander, S. Barlow, S.R. Marder, B. Kippelen, Org. Electron 13 (2012) 1166.
[21] H.G. Jeong, B. Lim, S.I. Na, K.J. Baeg, J. Kim, J.M. Yun, D.Y. Kim, Macromol. Chem. Phys. 212 (2011) 2308.
[22] Y. Lu, H. Chen, X. Hau, X. Hu, S.C. Ng, Synth. Met. 160 (2010) 1438.
[23] Y.A. Udum, H.B. Yıldız, H. Azak, E. Sahin, O. Talaz, A. Çırpan, L. Toppare, J. App. Polym. Sci. 131 (2014) 40701.
[24] A. Basudam, M. Sarmishta, Prog. Polm. Sci. 2 (2004) 699.
[25] A.T. Lawal, S.B. Adeloju, Biosens. Bioelectron. 15 (2013) 377.
[26] S. Soylemez, F. Ekiz Kanik, M. Ileri, S.O. Hacioglu, L. Toppare, Talanta 118 (2014) 84.
[27] Y. Xian, Y. Hu, F. Liu, Y. Xian, H. Wang, L. Jin, Biosens. Bioelectron. 211 (2006) 1996.
[28] E. Baskurt, F. Ekiz, D. Odaci Demirel, S. Timur, L. Toppare, Colloids Surf. B 97 (2012) 13.
[29] M. Dervisevic, E. Dervisevic, M. Senel, E. Cevik, H.B. Yildiz, P. Camurlu, Enzyme Microb. Technol. 102 (2017) 53.
[30] H.B. Yildiz, S. Kiralp, L. Toppare, Y. Yagci, K. Ito, Mater. Chem. Phys. 100 (2006) 124.
[31] H. Yoon, Nanomaterials 3 (2013) 524.
[32] M. Gerard, A. Chaubey, B.D. Malhotra, Biosens. Bioelectron. 17 (2002) 345.
[33] H. Azak, S. Kurbanoglu, H.B. Yildiz, S.A. Ozkan, J. Electroanal. Chem. 770 (2016) 90.
[34] O. Turkarslan, S. Kayahan, L. Toppare, Sensors Actuators B Chem. 136 (2009) 484.
[35] H. Azak, E. Guler, U. Can, D.O. Demirkol, H.B. Yildiz, O. Talaz, S. Timur, RSC Adv. 42 (2013) 19582.
[36] M. Dervisevic, E. Dervisevic, H. Azak, E. Cevik, M. Şenel, H.B. Yildiz, Sensors Actuators B Chem. 225 (2016) 181.
[37] G. Oktem, A. Balan, D. Baran, L. Toppare, Chem. Commun. 47 (2011) 3933.
[38] S. Tuncagil, C. Ozdemir, D. OdaciDemirkol, S. Timur, L. Toppare, Food Chem. 127 (2011) 1317.
[39] F.B. Emre, F. Ekiz, A. Balan, S. Emre, S. Timur, L. Toppare, Sens. Actuators, B 158 (2011) 117.
[40] D. Zhai, B. Liu, Y. Shi, L. Pan, Y. Wang, W. Li, R. Zhang, G. Yu, ACS Nano 7 (2013) 3540.
[41] L. Ying, E.T. Kang, K.G. Neoh, J. Membr. Sci. 208 (2002) 361.
[42] H.B. Yildiz, D.O. Demirkol, S. Sayin, M. Yilmaz, O. Koysuren, M. Kamaci, J. Macromol. Sci. Part A Pure Appl. Chem. 50 (2013) 1075.
[43] H.B. Yildiz, S. Kiralp, L. Toppare, Y. Yagci, Int. J. Biol. Macromol. 37 (2005) 174.